

Estimation of primaries by sparse inversion from passive seismic data

G. J. A. van Groenestijn¹ and D. J. Verschuur¹

ABSTRACT

For passive seismic data, surface multiples are used to obtain an estimate of the subsurface responses, usually by a crosscorrelation process. This crosscorrelation process relies on the assumption that the surface has been uniformly illuminated by subsurface sources in terms of incident angles and strengths. If this is not the case, the crosscorrelation process cannot give a true amplitude estimation of the subsurface response. Furthermore, cross terms in the crosscorrelation result are not related to actual subsurface inhomogeneities. We have developed a method that can obtain true amplitude subsurface responses without a uniform surface-illumination assumption. Our methodology goes beyond the crosscorrelation process and estimates primaries only from the surface-related multiples in the available signal. We use the recently introduced estimation of primaries by sparse inversion (EPSI) methodology, in which the primary impulse responses are considered to be the unknowns in a large-scale inversion process. With some modifications, the EPSI method can be used for passive seismic data. The output of this process is primary impulse responses with point sources and receivers at the surface, which can be used directly in traditional imaging schemes. The methodology was tested on 2D synthetic data.

INTRODUCTION

In passive seismics, no controlled sources such as airguns, explosives, or vibrator trucks are used. Instead, passive sources are used such as mini earthquakes within the subsurface of the earth (for example, from reservoir rocks cracking due to fluid-pressure changes during production) or heavy traffic on the surface. We will compare the passive data model with the primary-multiple model and demonstrate that crosscorrelating data, as is usually done in seismic interferometry (see, e.g., Claerbout, 1968; Schuster, 2001; Shapiro and Campillo, 2004; Wapenaar, 2004; Wapenaar et al., 2004; Snieder et

al., 2006; Dellinger and Yu, 2009; Draganov et al., 2009), is only the first step in a modified version of the recently introduced estimation of primaries by sparse inversion (EPSI) method (van Groenestijn and Verschuur, 2009a). A framework to describe active and passive seismic data (Berkhout and Verschuur, 2009) proposes to find the primary impulse responses via an inversion method. As it turns out, the modified EPSI algorithm does just that.

The EPSI method was introduced to avoid the subtraction of predicted multiples from actively acquired surface seismic data and uses a large-scale inversion process, in which the primaries are considered to be the unknowns. By iterative updating of the primary impulse responses, using a sparseness constraint, these primaries and their corresponding surface multiples are matched to the total data. Thus, adaptive subtraction is completely avoided because this process explains primaries and multiples simultaneously. Furthermore, van Groenestijn and Verschuur (2009a) show the merits of this method for near-offset reconstruction. In this paper, we extend the application of EPSI to passive seismic data.

An advantage of estimating primary impulse responses compared to crosscorrelating data is that the surface no longer must be illuminated uniformly by the passive sources in terms of incident angles and strengths. Wapenaar et al. (2008) also describe a method that has the same favorable characteristic. However, they assume that the direct signal arriving from all passive sources is known, which makes it possible to obtain the total impulse responses (including multiples) through multidimensional deconvolution. In this paper, we have assumed that this direct arrival is unknown.

First, we will discuss the primary-multiple model for standard seismic acquisition and briefly review the EPSI method. Then we will show that the primary-multiple model can be easily extended to the situation of passive seismic data. After some modifications to the EPSI algorithm, it can reconstruct primaries from passive data. The methodology is illustrated for 2D synthetic data.

EPSI

In the detail-hiding operator notation for 2D data (Berkhout, 1982), a bold quantity represents a prestack data volume for one frequency, columns represent monochromatic shot records, and rows

Manuscript received by the Editor 7 September 2009; revised manuscript received 29 December 2009; published online 31 August 2010.
¹Delft University of Technology, Delft, The Netherlands. E-mail: G.J.A.vanGroenestijn@tudelft.nl; D.J.Verschuur@tudelft.nl.

© 2010 Society of Exploration Geophysicists. All rights reserved.

represent monochromatic common receiver gathers. With the use of this notation, we can express the upgoing data acquired in controlled-source seismic exploration at the surface \mathbf{P}^- as

$$\mathbf{P}^- = \mathbf{X}_0 \mathbf{S}^+ + \mathbf{X}_0 \mathbf{R}^\cap \mathbf{P}^-, \quad (1)$$

where the primary impulse responses \mathbf{X}_0 multiplied with the source properties \mathbf{S}^+ equal the primaries $\mathbf{P}_0 = \mathbf{X}_0 \mathbf{S}^+$. Note that what is called “primaries” in this paper refers to all events that did not reflect at the surface, which includes internal multiples. The matrix multiplication of \mathbf{X}_0 with the reflection operator at the surface from below \mathbf{R}^\cap and the total data result in the surface multiples $\mathbf{M} = \mathbf{X}_0 \mathbf{R}^\cap \mathbf{P}^-$.

If we take $\mathbf{S}^+ = S(\omega) \mathbf{I}$, meaning a constant source wavelet for all shots and neglecting directivity of the source array, equation 1 becomes

$$\mathbf{P}^- = \mathbf{X}_0 S + \mathbf{X}_0 \mathbf{R}^\cap \mathbf{P}^-. \quad (2)$$

We aim at an inversion process that estimates $\hat{\mathbf{X}}_0$ and \hat{S} so that the total upgoing data \mathbf{P}^- are explained according to equation 2. Thus, the objective function J is introduced as

$$J_i = \sum_{\omega} \sum_{j,k} |\mathbf{P}^- - \hat{\mathbf{X}}_{0,i} \hat{S}_i - \hat{\mathbf{X}}_{0,i} \mathbf{R}^\cap \mathbf{P}^-|_{j,k}^2, \quad (3)$$

where i denotes the iteration, $\sum_{j,k}$ indicates a summation over all the elements of the matrix, and \sum_{ω} indicates a summation over all the frequencies. Van Groenestijn and Verschuur (2009a) introduce EPSI to solve this problem by an iterative optimization process. We assume that $\mathbf{R}^\cap = -\mathbf{I}$. In the first iteration of this algorithm we set the values of $\hat{\mathbf{X}}_0$ and \hat{S} to zero.

First, $\hat{\mathbf{X}}_0$ is updated. The update $\Delta \mathbf{X}_0$ is a steepest descent step

$$\Delta \mathbf{X}_0 = (\mathbf{P}^- - \hat{\mathbf{X}}_{0,i} \hat{S}_i - \hat{\mathbf{X}}_{0,i} \mathbf{R}^\cap \mathbf{P}^-) (\hat{S}_i \mathbf{I} + \mathbf{R}^\cap \mathbf{P}^-)^H, \quad (4)$$

where $(\hat{S}_i \mathbf{I} + \mathbf{R}^\cap \mathbf{P}^-)^H$ is the complex adjoint of $(\hat{S}_i \mathbf{I} + \mathbf{R}^\cap \mathbf{P}^-)$. The term $(\mathbf{P}^- - \hat{\mathbf{X}}_{0,i} \hat{S}_i - \hat{\mathbf{X}}_{0,i} \mathbf{R}^\cap \mathbf{P}^-)$ can be seen as the unexplained data or the residual. Because $\hat{\mathbf{X}}_0$ and \hat{S} are zero in the first iteration step, the first step equals a multidimensional correlation of the data with itself, $\mathbf{P}^- (\mathbf{R}^\cap \mathbf{P}^-)^H$.

To constrain the inversion process, van Groenestijn and Verschuur (2009a) propose to enforce sparseness on the update of $\hat{\mathbf{X}}_0$, which is achieved in a separate step. This proposition assumes that \mathbf{X}_0 can be represented in the time domain by a limited number of spikes with large amplitudes (from the major reflecting boundaries) and many small amplitude spikes (from all other events). A window is placed over the update of $\hat{\mathbf{X}}_0$ in the time domain and the strongest event(s) per trace is (are) selected. By increasing the size of the window in each iteration convergence is improved. The window should

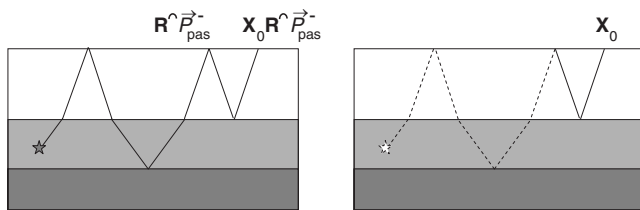


Figure 1. (a) Raypath of the direct arrival of the subsurface signal and its surface multiples. (b) An autocorrelation of the total data among others, “removes” the first part of the raypath (dashed line), resulting in a primary impulse-response estimation (solid line).

exclude events not associated with primaries as much as possible. Especially the strong first-order water-bottom multiple should be excluded in the first iteration. The window must also exclude artifacts that appear before the first arrivals. Next, the sparse update $\Delta \hat{\mathbf{X}}_0$ is added to the primary impulse response

$$\hat{\mathbf{X}}_{0,i+1} = \hat{\mathbf{X}}_{0,i} + \alpha \Delta \hat{\mathbf{X}}_0, \quad (5)$$

where α is a positive frequency-independent factor that scales the update step. Scale factor α is chosen so that the objective function value decreases.

The update of \hat{S} is executed in the same way as the update of $\hat{\mathbf{X}}_0$:

$$\Delta S = \hat{\mathbf{X}}_{0,i+1}^H (\mathbf{P}^- - \hat{\mathbf{X}}_{0,i+1} \hat{S}_i - \hat{\mathbf{X}}_{0,i+1} \mathbf{R}^\cap \mathbf{P}^-). \quad (6)$$

From the full matrix ΔS , the diagonal elements are selected and averaged to obtain the scalar ΔS . Here, ΔS is brought to the time domain, where its length is limited. After that, the update is scaled to ensure that the next objective function of equation 3 is lower than the previous one.

These two update steps are repeatedly applied until no more (visible) events are left in the residual.

PASSIVE SEISMIC DATA

Next, the passive seismic data situation is considered. The main difference with the surface seismic data is that primary reflection responses from controlled sources are not present. Instead, there is a direct arrival from passive sources toward the surface. This direct arrival is the cause of a series of surface multiples. This can be described in a model similar to that of equation 2:

$$\vec{\mathbf{P}}_{\text{pas}}^- = \vec{\mathbf{P}}_{\text{dir}}^- + \mathbf{X}_0 \mathbf{R}^\cap \vec{\mathbf{P}}_{\text{pas}}^-, \quad (7)$$

where $\vec{\mathbf{P}}_{\text{pas}}^-$ is the measured upgoing wavefield and $\vec{\mathbf{P}}_{\text{dir}}^-$ is the direct signal arriving from all passive sources in the subsurface (see also Berkhout and Verschuur, 2009). Here, $\vec{\mathbf{P}}_{\text{pas}}^-$ and $\vec{\mathbf{P}}_{\text{dir}}^-$ are each described by a column vector (i.e., one shot record but with a very long time duration). The first term in equation 7 cannot be expressed in terms of primary impulse responses but the second term $\mathbf{X}_0 \mathbf{R}^\cap \vec{\mathbf{P}}_{\text{pas}}^-$ equals the multiple term in the primary-multiple model (equation 2). Rearranging terms leads to $\vec{\mathbf{P}}_{\text{dir}}^- = \vec{\mathbf{P}}_{\text{pas}}^- - \mathbf{X}_0 \mathbf{R}^\cap \vec{\mathbf{P}}_{\text{pas}}^-$. The sparseness constraint on \mathbf{X}_0 in the time domain is no longer enough to solve the two unknowns $\vec{\mathbf{P}}_{\text{dir}}^-$ and \mathbf{X}_0 ; therefore, an extra constraint is required and we assume that $\vec{\mathbf{P}}_{\text{dir}}^-$ has minimum energy. Thus, the objective function to minimize is now

$$J_i = \sum_{\omega} \sum_{j,k} |\vec{\mathbf{P}}_{\text{pas}}^- - \hat{\mathbf{X}}_{0,i} \mathbf{R}^\cap \vec{\mathbf{P}}_{\text{pas}}^-|_{j,k}^2. \quad (8)$$

Again, we assume that $\mathbf{R}^\cap = -\mathbf{I}$. The algorithm starts with setting $\hat{\mathbf{X}}_0$ to zero. The update of $\hat{\mathbf{X}}_0$ is given by

$$\Delta \mathbf{X}_0 = (\vec{\mathbf{P}}_{\text{pas}}^- - \hat{\mathbf{X}}_{0,i} \mathbf{R}^\cap \vec{\mathbf{P}}_{\text{pas}}^-) (\mathbf{R}^\cap \vec{\mathbf{P}}_{\text{pas}}^-)^H. \quad (9)$$

Note that $\Delta \mathbf{X}_0$ is again a full matrix. For the first iteration, this update is equal to the multidimensional correlation of the data with itself $\vec{\mathbf{P}}_{\text{pas}}^- (\mathbf{R}^\cap \vec{\mathbf{P}}_{\text{pas}}^-)^H$, as used in seismic interferometry (see, e.g., Wapenaar et al., 2004). Figure 1 illustrates how the correlation $(\vec{\mathbf{P}}_{\text{pas}}^- - \hat{\mathbf{X}}_{0,i} \mathbf{R}^\cap \vec{\mathbf{P}}_{\text{pas}}^-) (\mathbf{R}^\cap \vec{\mathbf{P}}_{\text{pas}}^-)^H$ removes the first part of the raypath, resulting in the path of the primary impulse response. Note that the correlation will also create artifacts and give incorrect amplitudes for the

primary impulse responses. These artifacts and incorrect amplitudes will influence the residual and therefore are dealt with in later iterations. Next, a window is placed over the update $\Delta \mathbf{X}_0$ in the time domain and sparseness is imposed on $\Delta \mathbf{X}_0$. Note that the choice of the window for the passive data case is less trivial than for the active data case. For active data, the observed shallow events such as the water-bottom reflection will help to optimally design a window that does not pick up the first water-bottom multiple in the first iterations. For passive data, this prior knowledge is not present and needs to be extracted from the crosscorrelation result. The strongest primaries need to be identified and the window must be based on that interpretation. Equation 5 is used to find $\hat{\mathbf{X}}_{0,i+1}$ so that equation 8 is minimized.

In each iteration, \mathbf{X}_0 is updated. The iterations are stopped when no more (visible) changes are observed in the residual. What is left in the residual is an estimate of \hat{P}_{dir}^- . Note that EPSI applied to passive data does neither estimate the source signals emitted by the passive sources nor assume their properties.

For EPSI applied to actively and passively acquired data, only the upgoing wavefields are used. For land/ocean-bottom-cable (OBC) data, we assume that surface/interface waves are removed by filter-

ing and multicomponent measurements are used to obtain an up/down separation. For marine data, it means that deghosting is applied.

RESULTS

The proposed inversion method is tested on a synthetic data set. The 2D two-reflector model used to create these data can be seen in Figure 2. Eighty-one subsurface sources, which emit small bursts, were placed randomly in an area below the second reflector.

The first update of \mathbf{X}_0 before the application of the sparseness constraint is shown in Figure 3a. Note again that this is the traditional interferometry result obtained by crosscorrelating the traces of the passive data. Figure 3b shows the first update of \mathbf{X}_0 after applying sparseness. How the estimation of the primary impulse responses develops during the iterations can be seen in Figure 3c-e. For display purposes, the spiky primary impulse response estimates have been convolved with an arbitrary wavelet.

Figure 4d-f shows the primary impulse responses obtained after 30 iterations. Note the reduction of crossterms, which is visible in the traditional interferometric result (Figure 5d-f) after 30 iterations of our algorithm (Figures 4d-f). For comparison, the modeled primaries from a standard reflection survey at the surface have been displayed in Figure 4a-c. Note that the use of a sparseness constraint yields small discontinuities at various locations. Modeled shot gathers are displayed in Figure 5a-c for comparison of the interferometric result with the total (primaries and multiples) subsurface response.

Also, note that not all angles are present in the estimated primary impulse responses. This can be understood because the surface is not illuminated with all angles and therefore the surface reflection cannot illuminate the subsurface under all angles. The illumination angles per offset can be estimated from the “crosses” at and around offset = 0 and $t = 0$ in the correlation $\hat{P}_{pas}^-(\mathbf{R} \cap \hat{P}_{pas}^-)^H$. In Figure 5g-i, the interferometry results are plotted in the τ - p domain. The cross in Figure 5e is the sum of the correlations of each local plane wave arriving at receiver position $x = 1000$ m. Correlating the plane-wave event in the trace $x = 1000$ m with itself will result in a peak at $t = 0$.

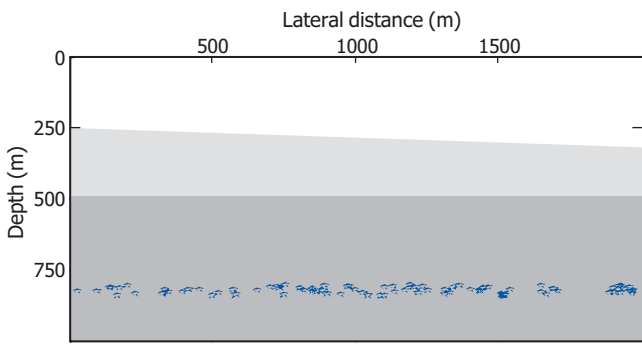


Figure 2. The subsurface model used to generate the passive seismic data. It shows the location of the passive sources below the second reflector. The top layer is water.

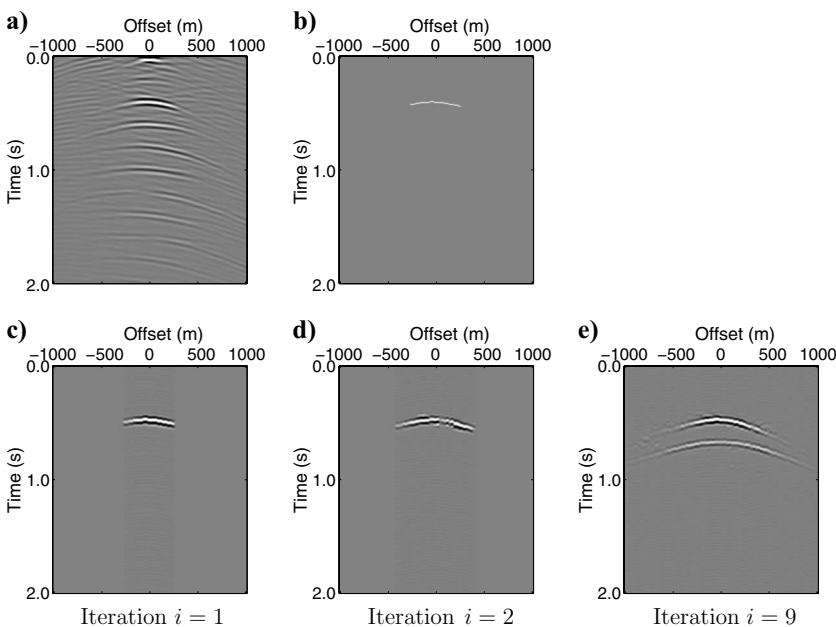


Figure 3. (a) The first update of the primary impulse responses before windowing and making it sparse for a “shot” at receiver position 1000 m. Note that this represents the traditional interferometry result. (b) The result of (a) after it is windowed and made sparse. (c-e) The estimated primary impulse response for different iterations, convolved with an arbitrary wavelet for display purposes.

Correlating the plane-wave event in trace $x = 1000$ m with the same plane-wave event in trace $x = 1025$ m will show a peak with a time shift inversely proportional to the apparent velocity of the plane-wave event. Because the lowest apparent velocity in our model is the water velocity (1500 ms^{-1}), the steepest angle in the crosses can be

$1/(1500 \text{ ms}^{-1}) = 66 \cdot 10^{-5} \text{ sm}^{-1}$. As can be seen from the event at $\tau = 0$ in Figure 5h, the ray parameter associated with the steepest angle in the water layer is missing. Figure 6a displays the zero offset section of the interferometric result and Figure 6b displays the zero

Figure 4. Modeled primaries obtained from standard acquisition belonging to a shot at receiver position: (a) 500 m, (b) 1000 m, (c) 1500 m. (d-f) Estimated primary impulse responses for the same positions via EPSI obtained from passive data, displayed with an arbitrary wavelet.

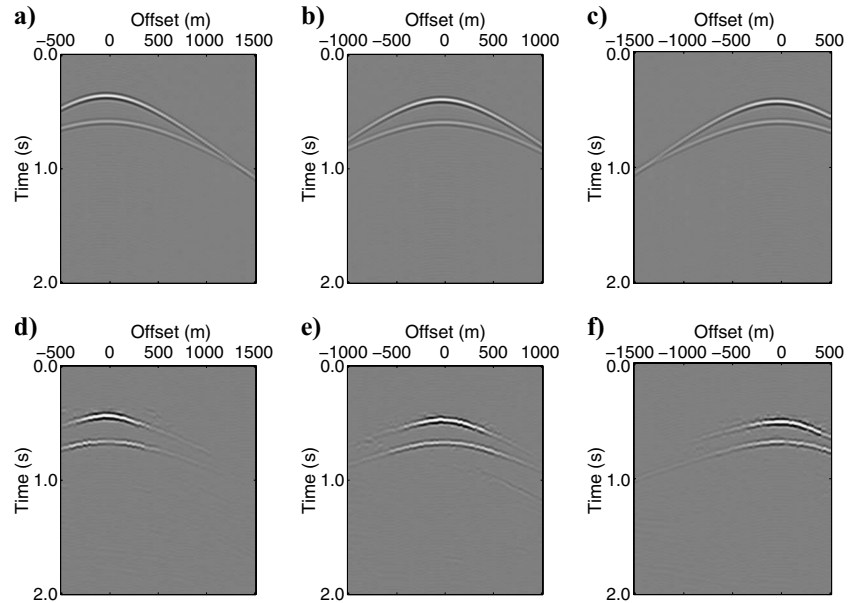
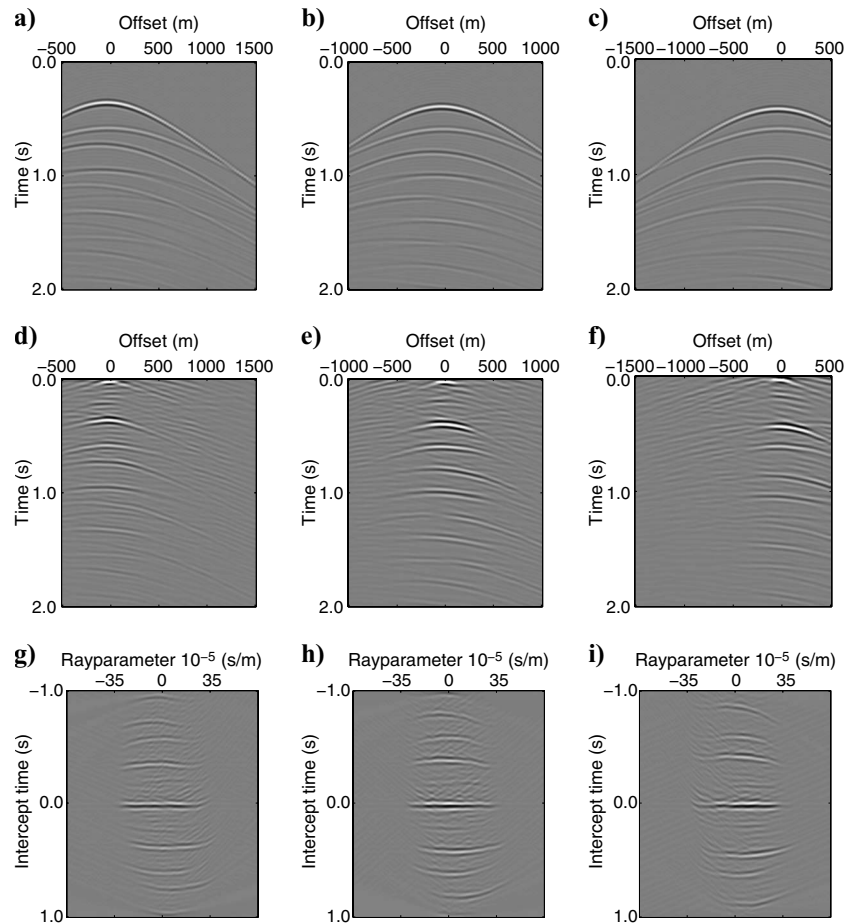


Figure 5. Modeled shot gathers obtained from standard acquisition belonging to a shot at receiver position: (a) 500 m, (b) 1000 m, (c) 1500 m. (d-f) The interferometric result obtained from the same passive data as used in Figure 4. (g-i) The τ - p transforms of the interferometric results. Note that these displays are centered around zero time.



offset section of the estimated primary impulse responses convolved with the same arbitrary wavelet, as in Figure 4d-f.

As stated earlier, one interesting aspect of our approach is that it can obtain \mathbf{X}_0 also in the case when the passive sources have different strengths and nonuniform illumination angles in contrast to the traditional crosscorrelation method. Wapenaar et al. (2008) also describe a method that has the same favorable characteristic; however, they assume that \tilde{P}_{dir}^- is known. In this paper, we have assumed that \tilde{P}_{dir}^- is unknown; however, if (parts of) \tilde{P}_{dir}^- are known they could be subtracted from $(\tilde{P}_{\text{pas}}^- - \mathbf{X}_0 \mathbf{R} \tilde{P}_{\text{pas}}^-)$ in equation 8. In that case, the objective function will get (closer to) zero. Furthermore, note that our method provides the primary impulse responses instead of the total impulse responses that include the surface multiples.

We test the case of passive sources with different strengths for the subsurface model of Figure 2. We use the same subsurface source locations except this time the source strengths are no longer equal but increase linearly as a function of the horizontal source position so a subsurface source at $x = 2000$ m is four times as strong as a source at $x = 0$ m. Figure 6c shows the zero offset section of the interferometric result $\tilde{P}_{\text{pas}}^- (\mathbf{R} \tilde{P}_{\text{pas}}^-)^H$. Clearly, the influence of the different source strengths can be seen. Figure 6d shows the zero offset section of the EPSI result. As expected, no influence of the different source strengths can be observed.

Next, we test the case in which the area of subsurface sources is limited horizontally. For this, we use the same subsurface model of Figure 2 but this time we only take the subsurface sources between $x = 800$ m and $x = 1200$ m. Figure 7a-c shows the interferometric result of these data; Figure 7d-f shows the EPSI result. Apart from a small leakage in the EPSI result, we can see that the events that are visible are in the right locations. This is in contrast to the crosscorrelation result that also shows events in the wrong locations. Compared to Figure 4d-f, fewer angles are present in the primary impulse-response estimates but this can be understood by the fact that the illumination angles of the surface have been reduced. Thus, this is not a limitation of our method but an intrinsic limitation of the

data. The limitation becomes visible in the τ - p plots in Figure 7g-i.

Finally, we test the EPSI method with a more complex subsurface model (Figure 8a). Three hundred and sixty-one subsurface sources (equal in source strengths) are randomly distributed in the area between depths of 980 m and 1045 m and between lateral distances of 0 m and 5400 m (Figure 8b). Figure 9a shows a part of the input data. The events in the figure are generated by one subsurface source. The EPSI method has explained the multiples $\hat{\mathbf{X}}_0 \mathbf{R} \tilde{P}_{\text{pas}}^-$ (Figure 9b) in these data. The unexplained data (Figure 9c) are considered to be the direct arrival \tilde{P}_{dir}^- . Note that the direct arrival consists of several events. In this case, all direct-arrival events come from one source but we should realize that they also could have come from different sources.

Figure 10d-f shows the obtained primary impulse responses. For comparison, the modeled primaries from a standard acquisition (Figure 10a-c) and the interferometric result, being the first step of our inversion algorithm (Figure 10g-i), are shown. It is clearly visible that not all angles are present in the estimates. This can be understood by the fact that the surface points are not illuminated by all angles, as can be seen in Figure 10j and k. Apart from the discontinuity due to missing illumination angles it is clearly visible that the primary impulse responses are discontinuous in some other parts. The EPSI method works with placing spikes (see Figure 3b). For a simple subsurface model as in Figure 2, this happened in a continuous manner, but for a more complex model some parts in the end result are discontinuous. However, the multiples that are created through a multidimensional convolution and summation $\hat{\mathbf{X}}_0 \mathbf{R} \tilde{P}_{\text{pas}}^-$, these primary impulse responses are continuous, as can be seen in Figure 9b. The stack of the primary impulse responses is also continuous (Figure 11b). For comparison, the stacked true primaries from standard acquisition (Figure 11a), the stacked total data from standard acquisition (Figure 11c), and the stacked interferometric result (Figure 11d) are shown as well. It is interesting that the EPSI result compared

Figure 6. Zero offset section of (a) the interferometric result and (b) the EPSI result for data from subsurface sources that are equal in strength. Zero offset section of (c) the interferometric result and (d) the EPSI result for data from subsurface sources that vary in source strengths from left to right with a factor of four. Note that the EPSI result is insensitive to the source-strength variations.

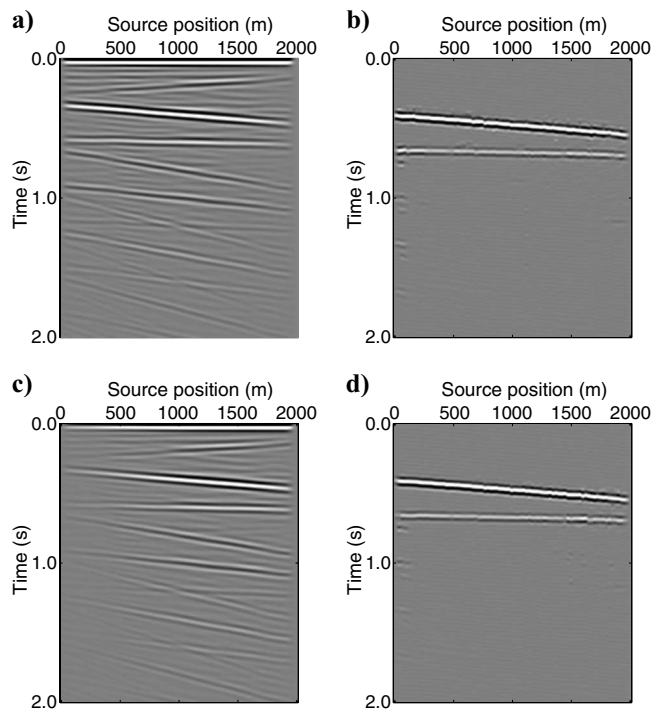


Figure 7. The EPSI result for data with a limited horizontal range of subsurface sources for a “shot” at receiver position: (a) 500 m, (b) 1000 m, (c) 1500 m. (d-f) The interferometric result on the same data. (g-i) The τ - p transforms of the interferometric result.

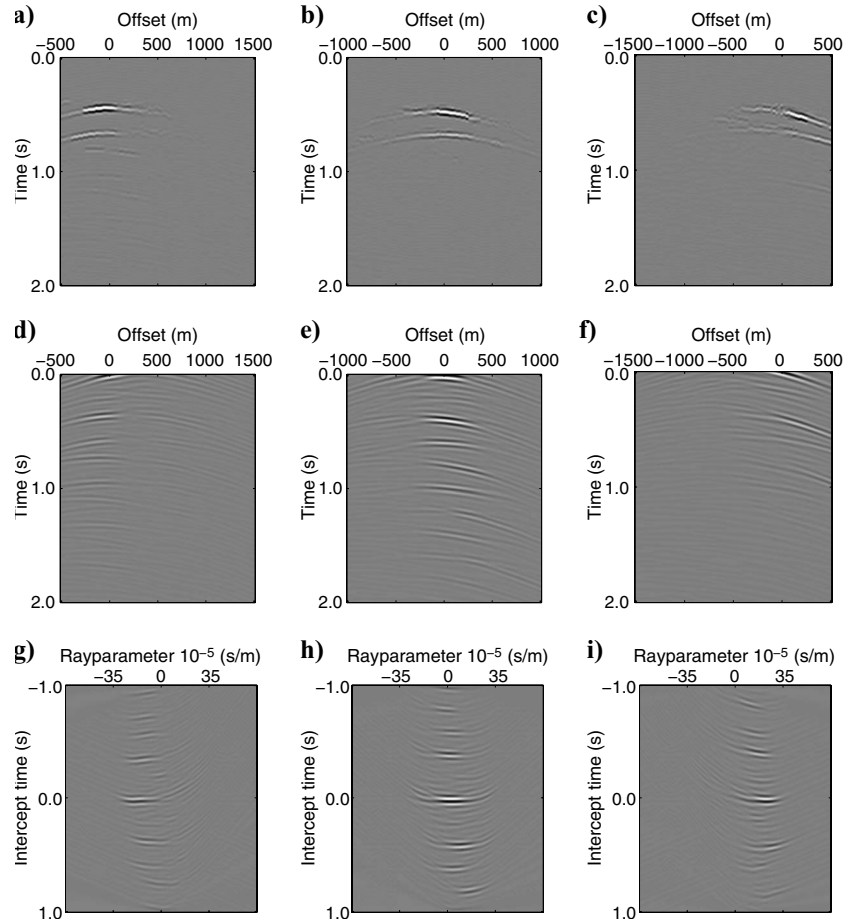


Figure 8. (a) Synthetic salt model with water as the top layer. The passive subsurface sources are randomly located between 980 and 1045 m depth over the full horizontal range. (b) The distribution of the passive subsurface sources.

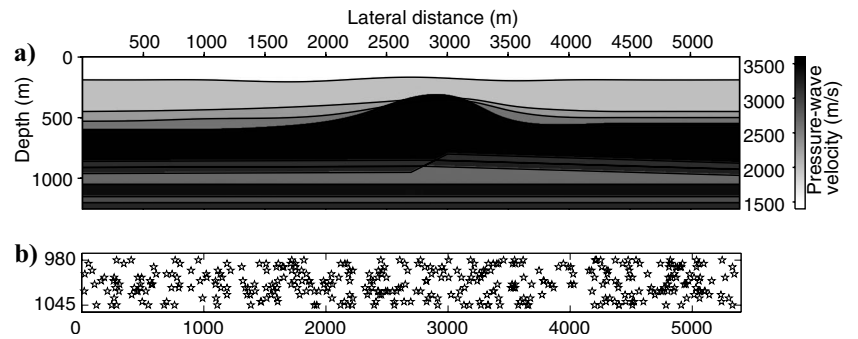
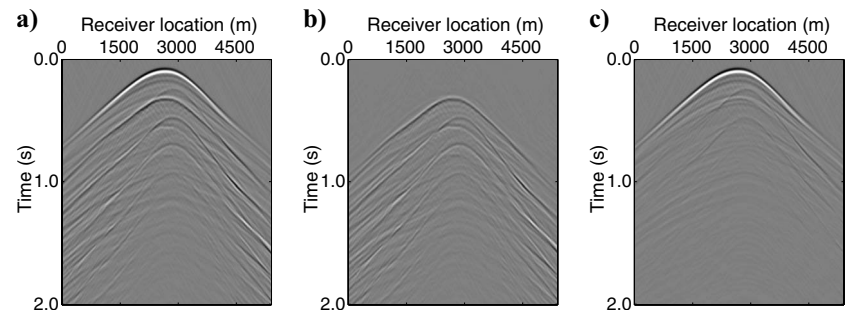


Figure 9. (a) Response of a subsurface source measured at the surface P_{pas}^- . The time $t = 0$ is arbitrary. (b) The estimated multiples $\hat{\mathbf{X}}_0 \mathbf{R} \hat{\mathbf{P}}_{pas}^-$. (c) The residual equals (a) the input data minus (b) the estimated multiples. The residual is an estimate of the direct arrival \hat{P}_{dir}^- .



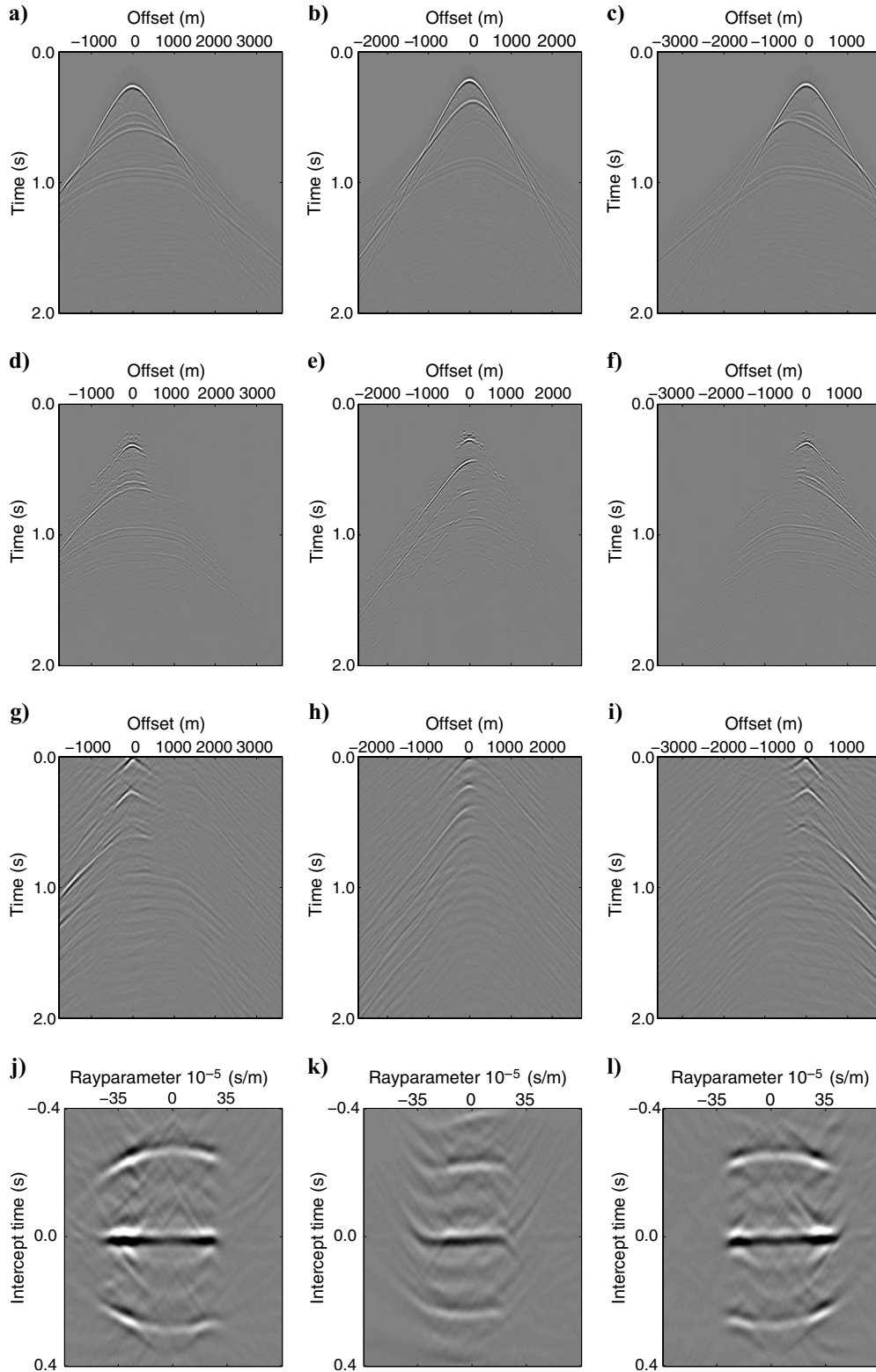


Figure 10. A shot gather obtained from standard acquisition belonging to a shot at receiver position: (a) 1800 m, (b) 2700 m, (c) 3600 m. (d-f) The estimated primary impulse responses via EPSI obtained from passive data with an arbitrary wavelet for the same positions. (g-i) The interferometric result for the same passive data. (j-k) The τ - p transforms of the interferometric result, displayed for a time window around $\tau = 0$.

to the correlation has high resolution. Note that EPSI and interferometry are able to obtain the diffraction energy.

DISCUSSION

An extra constraint can be added to the objective function in equation 8 to force events to be laterally more consistent. Taking into account that this constraint will also force true discontinuous events to be erroneously continuous, plus the fact that many processes that will follow primary estimation in the seismic processing chain are not hindered by discontinuity, one might decide to keep the discontinuous parts. Stacking is an example of a process that is not hindered by discontinuity, as is demonstrated in the stacked estimated primary impulse responses in Figure 11b. With respect to discontinuous events, it is interesting to note that in Lin and Herrmann (2009) the curvelet transform is combined with the EPSI algorithm for simultaneous source data. By minimizing the L1 norm of the estimated primary impulse responses in the curvelet domain, lateral continuity is improved.

We have no physical justification for the assumption that the direct arrivals have minimum energy but we would like to point out that more or less the same assumption is made in multiple elimination methods applied to actively acquired data such as SRME. In these multiple-elimination methods, the minimum energy of the primaries is assumed when the predicted multiples are adaptively subtracted from the data. For the most cases, this assumption results in a good primary estimation. However, in data sets where primaries and multiples overlap in the same way everywhere in the data, the assumption turns out to be invalid. The data from passive subsurface sources, however, might be found in a more favorable position with respect to the overlap between the direct arrival and the multiples. This is due to the fact that the variation in direct arrivals is bigger than the variation in primaries from actively acquired data; there-

fore, the direct arrivals and multiples overlap less in the same way everywhere in the data set.

It might give some insights to reorder equation 7 into

$$\vec{P}_{\text{pas}}^- - \vec{P}_{\text{dir}}^- = \mathbf{X}_0 \mathbf{R} \cap \vec{P}_{\text{pas}}^-, \quad (10)$$

In this way, we have a downgoing wavefield ($\mathbf{R} \cap \vec{P}_{\text{pas}}^-$), the consequences of this downgoing wavefield ($\vec{P}_{\text{pas}}^- - \vec{P}_{\text{dir}}^-$), and the primary impulse responses that connect both. The presence of the direct arrivals makes it impossible to obtain \mathbf{X}_0 by a multidimensional division of the upgoing wavefield by the downgoing as can be done for vertical seismic profile data (Ross and Shah, 1987), OBC data (Amundsen, 1999), or surface data (van Groenestijn and Verschuur, 2009a) but the inversion approach is in essence making this division. By looking at EPSI as a method that divides the upgoing by the downgoing wavefield, it becomes clear that the receivers do not have to be positioned at the surface. It also makes it easy to understand that the different source signatures in the passive data are divided out. It is interesting to see that the correlation approach has been applied in similar ways to virtual source data (Mehta et al., 2007), OBC data (Cao, 2009), and surface data (Claerbout, 1968). Here, the correlation of the upgoing wavefield with the downgoing is used to obtain an estimate of the total subsurface response. The similarities between approaches make it clear that the deconvolution and correlation approaches can benefit from each other.

The question is how well our method will behave on field data. The synthetic models that we have chosen have their random sources located in a small layer, thus mimicking reservoir rocks that crack during production. These microseismic events can be monitored (see, e.g., Maxwell and Urbancic, 2001). Current studies on field data, however, show that in practice applying the interferometric method is not trivial. Dellinger and Yu (2009) only manage to reconstruct Scholte waves from passive OBC data. This means that our method, which uses the crosscorrelation process as a first step, can-

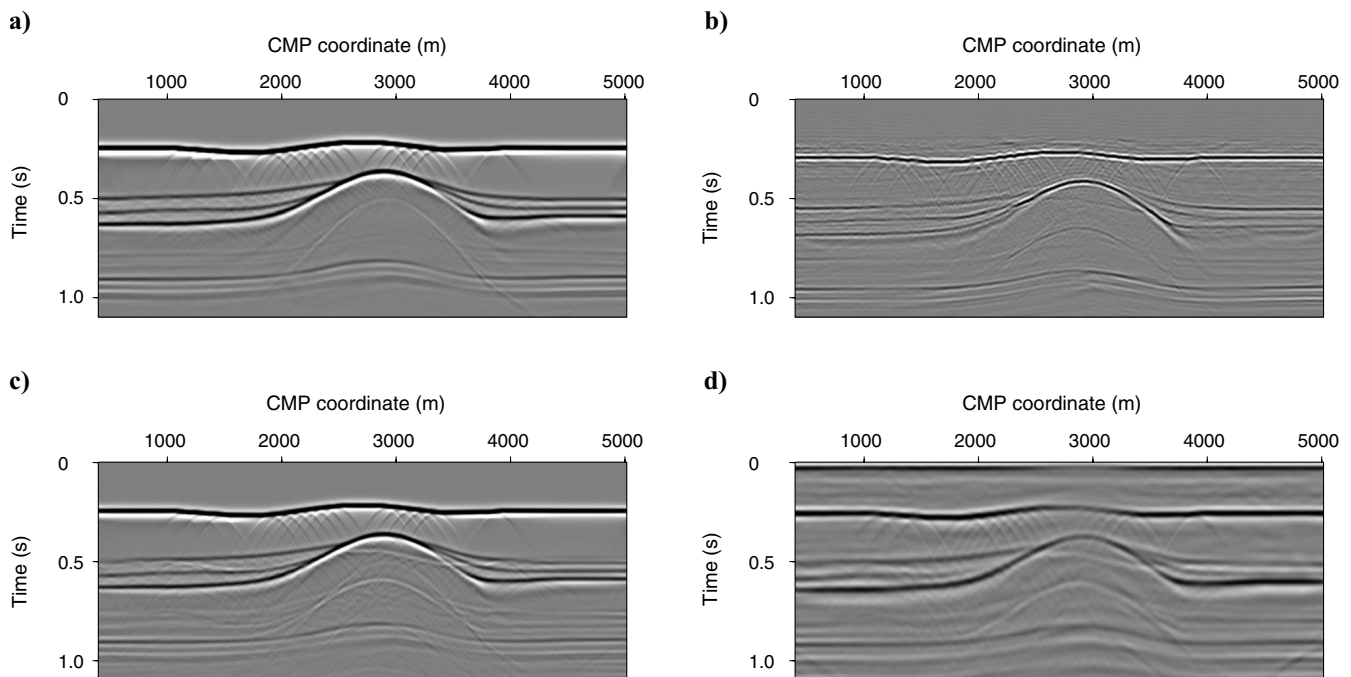


Figure 11. Stacks of (a) the true primaries obtained from standard acquisition, (b) the EPSI result on passive data, (c) the total data obtained from standard acquisition, and (d) the interferometric result on passive data.

not be used in such cases. Draganov et al. (2009) manage to reconstruct reflection energy only after preprocessing the passive data, including applying dip filters to remove the surface waves. For such data, our proposed method can be used. Using densely sampled passive receiver arrays will increase the chance of success of our method, because this allows better preprocessing such as aliasing-free dip filters.

It is known that attenuation is a problem for interferometry (Rui-grok et al., 2008). The EPSI method, however, can handle attenuation and will estimate it as part of the impulse response. This means that dispersion effects, for example, become visible at later arrival times, meaning that EPSI needs a few spikes to describe each event at later times, requiring more iterations in the process. In van Groenestijn and Verschuur (2009b), EPSI is applied to two marine field data sets and demonstrates that the attenuation of higher frequencies will slow down the convergence of EPSI because it will create an X_0 that is less spiky. However, the end result is not affected by it.

The EPSI method can be of great value for reservoir monitoring through passive acquisition. The primary impulse responses are a function of the (changing) subsurface and not of the subsurface source strengths. Moreover, the primary impulse responses estimated by a passive acquisition can be combined with the primary impulse responses obtained by EPSI from a standard acquisition. Thus, EPSI is a very open method in the sense that it is easy to build in other applications, such as the reconstruction of missing near offsets (see van Groenestijn and Verschuur, 2009a). Therefore, we think that EPSI can also be reformulated to incorporate the estimation of the direct arrivals (shown in Figure 9c) in equation 8.

CONCLUSION

In this paper, we present the extension of EPSI to the situation of passive seismic data. The EPSI method uses the result of the cross-correlation process that is usually applied to passive data as input of an inversion process that will provide the impulse responses of the subsurface. Compared to the crosscorrelation method, our proposed method will remove the spurious correlation events and end up with primaries only. Furthermore, the obtained primary impulse responses are true amplitude without the sensitivity to the distribution and strengths of the various noise sources, as observed in crosscorrelation results.

ACKNOWLEDGMENTS

The authors thank the sponsors of the DELPHI consortium for the support of this research and for the stimulating discussions at the

consortium meetings. Professor A. J. Berkhouit is thanked for the discussions that led to the application of EPSI to passive data. Xander Campman, Sjoerd de Ridder, and an anonymous reviewer are thanked for their suggestions that have improved the paper.

REFERENCES

- Amundsen, L., 1999, Free-surface multiple attenuation of four-component (4C) sea floor recordings: 69th Annual International Meeting, SEG, Expanded Abstracts, 868–871.
- Berkhouit, A. J., 1982, Seismic migration, imaging of acoustic energy by wave field extrapolation: Theoretical aspects: Elsevier.
- Berkhouit, A. J., and D. J. Verschuur, 2009, Integrated imaging with active and passive seismic data, SEG, Expanded abstracts, 1592–1596.
- Cao, W., 2009, Interferometric interpolation of 3D obs data: 79th Annual International Meeting, SEG, Expanded Abstracts, 3148–3152.
- Claerbout, J. F., 1968, Synthesis of a layered medium from its acoustic transmission response: *Geophysics*, **33**, 264–269.
- Dellinger, J. A., and J. Yu, 2009, Low-frequency virtual point-source interferometry using conventional sensors: 71st Annual International Meeting, EAGE, Extended Abstracts.
- Draganov, D., X. Campman, J. Thorbecke, A. Verdel, and K. Wapenaar, 2009, Subsurface structure from ambient seismic noise: 71st Annual International Meeting, EAGE, Extended Abstracts, Z038.
- Lin, T. T., and F. J. Herrmann, 2009, Unified compressive sensing framework for simultaneous acquisition with primary estimation: 79th Annual International Meeting, SEG, Expanded Abstracts, 3113–3117.
- Maxwell, S. C., and T. I. Urbancic, 2001, The role of passive microseismic monitoring in the instrumented oil field: *The Leading Edge*, **20**, 636–639.
- Mehta, K., A. Bakulin, J. Sheiman, R. Calvert, and R. Snieder, 2007, Improving the virtual source method by wavefield separation: *Geophysics*, **72**, no. 4, V79–V86.
- Ross, W. S., and P. M. Shah, 1987, Vertical seismic profile reflectivity: Ups over downs: *Geophysics*, **52**, 1149–1154.
- Ruigrok, E., D. Draganov, and K. Wapenaar, 2008, Global-scale seismic interferometry: Theory and numerical examples: *Geophysical Prospecting*, **56**, 395–417.
- Schuster, G. T., 2001, Theory of daylight/interferometric imaging: Tutorial: 63rd Annual International Meeting, EAGE, Extended Abstracts, Session A-32.
- Shapiro, N., and M. Campillo, 2004, Emergence of broadband rayleigh waves from correlations of the ambient seismic noise: *Geophysical Research Letters*, **31**, L07614.
- Snieder, R., K. Wapenaar, and K. Lerner, 2006, Spurious multiples in seismic interferometry of primaries: *Geophysics*, **71**, no. 4, SI111–SI124.
- van Groenestijn, G. J. A., and D. J. Verschuur, 2009a, Estimating primaries by sparse inversion and application to near-offset data reconstruction: *Geophysics*, **74**, no. 3, A23–A28.
- , 2009b, Estimation of primaries and near-offset reconstruction by sparse inversion: Marine data applications: *Geophysics*, **74**, no. 6, R119–R128.
- Wapenaar, C. P. A., 2004, Retrieving the elastodynamic green's function of an arbitrary inhomogeneous medium by cross correlation: *Physical Review Letters*, **93**, 254301-1–254301-4.
- Wapenaar, C. P. A., J. W. Thorbecke, and D. Draganov, 2004, Relations between reflection and transmission responses of three-dimensional inhomogeneous media: *Geophysical Journal International*, **156**, 179–194.
- Wapenaar, K., J. van der Neut, and E. Ruigrok, 2008, Passive seismic interferometry by multidimensional deconvolution: *Geophysics*, **73**, no. 6, A51–A56.